A comprehensive, mechanistically detailed, and executable model of the Cell Division Cycle in *Saccharomyces cerevisiae*

Ulrike Münzner[1, 2], Edda Klipp[1] and Marcus Krantz[1]

1. Institute of Biology, Humboldt-Universität zu Berlin, Berlin, Germany

2. Bioinformatics Center, Institute for Chemical Research, Kyoto University, Uji, Japan

marcus.krantz@rxncon.org

ABSTRACT

Understanding how cellular functions emerge from the underlying molecular mechanisms is a key challenge in biology. This will require computational models, whose predictive power is expected to increase with coverage and precision of formulation. Genome-scale models revolutionised the metabolic field and made the first whole-cell model possible. However, the lack of genome-scale models of signalling networks blocks the development of eukaryotic whole-cell models. Here, we present a comprehensive mechanistic model of the molecular network that controls the cell division cycle in *Saccharomyces cerevisiae*. We use rxncon, the reaction-contingency language, to neutralise the scalability issues preventing formulation, visualisation and simulation of signalling networks at the genome-scale. We use parameter-free modelling to validate the network and to predict genotype-to-phenotype relationships down to residue resolution. This mechanistic genome-scale model offers a new perspective on eukaryotic cell cycle control, and opens up for similar models - and eventually whole-cell models - of human cells.

INTRODUCTION

Computational models provide powerful tools to study biological systems[1]. In particular, mechanistic models that explain cellular functions and phenotypes from molecular events are powerful tools to assemble knowledge into understanding. These models combine three functions: As integrated and internally consistent knowledge bases, as scaffolds for integration, analysis and interpretation of data, and as executable models. Their value arguably increases the more mechanistically detailed and comprehensive they are, culminating in the genome-scale mechanistic models of metabolism and the whole-cell model of *Mycoplasma genitalium*[2-4]. These models can be used to explain and predict perturbation responses and genotype-to-phenotype relationships, and whole cell models have the potential to revolutionise biology, biotechnology and biomedicine. However, to realise this potential, we must be able to build mechanistic genome-scale models of all cellular processes.

This has proven especially challenging for the cellular networks that process information (reviewed in 5,6). These networks encode information primarily through reversible state changes in their components, such as bonds or covalent modifications. Typically, these components interact with multiple partners and may be modified at multiple residues, and most of these bonds and/or modifications are not mutually exclusive. Consequently, there is a one-to-many relationship between empirical observables (*elemental states*), such as a specific bond or the modification status at a specific residue, and the possible configurations of the components (*microstates*). This leads to problems in most classical modelling formalism, where the resolution difference leads either to a loss of mechanistic detail (e.g. component level modelling) or to the combinatorial complexity (microstate modelling). The solution is to use a formalism with adaptive resolution, such as rule-based modelling languages (RBMLs)[7,8], the Entity Relationship diagrams of the Systems Biology Graphical Notation (SBGN-ER)[9] or rxncon, the reaction-contingency language[10] (reviewed in 11,12). However, the potential of these formalisms has yet to be realised in a comprehensive mechanistic model of a eukaryotic signalling system.

The eukaryotic cell division cycle (CDC) may be the most interesting - both medically and philosophically - of these systems, as it constitutes the very core of life as we know it. The CDC is best understood in baker's yeast, *Saccharomyces cerevisiae*: The rise and fall in activity of a single cyclin dependent kinase (CDK) suffices to drive the replication of DNA,

nuclear division (including duplication and separation of the spindle pole body (SPB, the yeast centrosome)) and cell morphology and division[13,14]. The molecular basis of cell cycle control has been studied since the 1970-ies with experimental[15] as well as computational[16-19] methods. However, even the largest executable models are far from genome-scale[19], and the exquisitely detailed map created in the process description diagram language (SBGN-PD[9]) cannot be executed[20]. To realise the potential of a mechanistic genome-scale model, we need to combine the features of all three efforts: The mechanistic precision in the molecular biology, the scope of the comprehensive maps, and the executability of the mathematical models.

Here, we present a mechanistic, executable and genome-scale model based on the network that controls and executes the cell division cycle in baker's yeast, *Saccharomyces cerevisiae*. We chose to build this model using rxncon, as it (similarly to RBMLs) has the adaptive resolution required to reconcile the necessary scalability and precision, and as a rxncon network (in contrast to a rule-based model (RBM)) can be compiled into and simulated as a parameter-free bipartite Boolean model (bBM)[21]. This scalable simulation method enables qualitative simulation of the cell cycle network, which is too large and/or has too many unknown parameter values (or truth tables) to be simulated with classical methods. We use bBM simulation to validate the wild-type model, prompting us to introduce a number of gap-filling changes to create a functional cell-cycle model. Interestingly, we find that the control network consists of three distinct regulatory modules that control and communicate via three independent replication cycles: DNA replication, SPB duplication and nuclear division, and cell division, and that only a hybrid model including both parts can mechanistically explain cell cycle control. Finally, we benchmark the model on a set of 85 mutants, capturing 63/85 phenotypes. Taken together, we show that it is possible to build, visualise and simulate mechanistic models of signal transduction systems at the genome-scale, and that system level function can be predicted from the level of molecular mechanisms without parametrisation or model training.

RESULTS

A comprehensive, mechanistic and executable model of a eukaryotic cell division cycle

We compiled literature knowledge into a mechanistically detailed model of cell division cycle control in baker's yeast (Figure 1a, Table S1, Sup File 1, Figure S1). We derived the knowledge from in-depth literature curation and formalised it in a rxncon model without any fitting or model optimisation. The model includes regulated expression and degradation of proteins, assembly and regulation of the cyclin dependent protein kinases Cdc28 (Cdk1) and Pho85 (Cdk5), and the regulation of DNA replication, SPB duplication and nuclear division, and cell polarity and morphogenesis. Each of these processes is defined – as far as empirical knowledge allows – down to the role of specific modifications and bonds at particular residues and domains. This molecular reaction network (MRN) accounts for 357 unique components. This number includes 229 proteins, and the genes and mRNAs of the 44 proteins for which we consider regulated expression and/or degradation. The model also includes 7 multimeric protein complexes (e.g. APC/C), 3 chromosomal features (e.g. the origins of replication), 29 kinase and phosphatase activities as target specific enzymes that remain to be mapped on one or more gene products (e.g. Sfi1PPT as an unidentified phosphatase (PPT) of Sfi1), and one small molecule: phosphatidylinositol (PI). These components take part in 790 elemental reactions that produce and consume 1238 elemental states, and that are regulated by 598 contingencies - several of which correspond to combinations of elemental states.

In addition to the MRN, we encode a coarse-grained model (CGM) of DNA replication, SPB duplication and the morphological cell cycle in 12 macroscopic reactions and 12 macroscopic states (Figure 1b). The macroscopic reactions respond to a series of inputs that constitutes outputs (observables) in the MRN. Conversely, the CGM outputs act as inputs to the MRN. The entire regulatory logic is encoded in a single hybrid rxncon model, encompassing 802 reactions and 972 lines of contingencies. The contingencies connect the MRN and CGM to each other. The contingencies also link to the five external inputs we consider to perturb the system allowing for further analysis: nutrients, pheromone, hydroxyurea (HU), latrunculin A (LatA) and nocodazole (NOC). The biology and implementation is described and visualised in detail in the supplementary documentation. The model accounts for all components to which we could assign a mechanistic function in the control of cell cycle division and, hence, it constitutes a first draft of a genome-scale mechanistic model (GSM) of eukaryotic cell division.

Building a mechanistic knowledge base at the genome scale

The GSM primarily constitutes a biological knowledge, which can be compiled into a mathematical model. In an iterative workflow[22], we extracted and evaluated empirical information, and formalised it as *elemental reactions* (e.g.: Cdc28 phosphorylates Sld2 at Threonine 84) and *contingencies* (e.g.: Cdc28 phosphorylates Sld2 at Threonine 84 only if Cdc28 is bound to Clb5 (or Clb6)). This type of mechanistic model puts high demands on data coverage and quality. We identified knowledge gaps, which forced specific gap-filling assumptions to create a fully connected model (Table S1). In addition, we made the general assumptions that all reversible covalent modifications and all synthesised components are turned over. This lead us to introduce a set of 28 undefined phosphatase activities to compensate for the fact that these reaction types are understudied[10]. These assumptions were lifted for highly stable proteins (e.g. Mcm2-Mcm7) and modifications turned over by degradation (e.g. Sic1 phosphorylation). Furthermore, we mapped the effect of localisation directly on the elemental states that are responsible for localisation changes (e.g: phosphorylation of Ace2 and Swi5 in the nuclear localisation signal directly regulates their promoter recruitment; Fig S3), bypassing the spatial description without compromising the regulatory logic. However, for most of the network we find biochemical (for reactions) or combinations of biochemical and genetic (for contingencies) data that can be formalised in the rxncon language using 14 elemental reaction types (Table S1), creating a mechanistically detailed knowledge base of the molecular network that controls and executes the cell division cycle.

Insights at the genome scale: Three independent replication programs

The GSM contains the current mechanistic knowledge on information transfer and, hence, connections represent direct and functional connections *in vivo*. Conversely, a lack of connection implies that no (known) direct and/or functional connection exists. In particular, there is very little interaction between the three duplication cycles that execute DNA replication (DNA), nuclear division (ND) comprised of SPB duplication and nuclear division itself, and cell division (CD) involving budding, morphology and cytokinesis outside of mitosis. While the lack of direct mechanistic connections between the cycles may reflect

missing knowledge, the GSM predicts that these cycles constitute distinct programs that can be executed independently through the appropriate adaptation of (the state of) the regulatory network. Such uncoupling has been observed in eukaryotic cells, leading to ploidy shifts, multinucleate cells, or cells without nuclei. The perhaps most prominent example of the modularity of these processes is meiosis, where a single DNA replication (pre-meiotic S-phase) is followed by two rounds of nuclear division (meiosis I + II) without any cell division[23]. Hence, the CDC consists of three independent replication cycles; DNA replication, nuclear division and cell division.

Mechanistic modularity: The CDC control network is not a cycle but three major checkpoints

We made a number of striking observations in the model building process. While we only used previously published data, the assembly into a holistic picture of the assembled knowledge highlighted features that were not obvious from the modules themselves. In particular, the regulatory network controlling the cell division cycle does not in itself form a cycle. Instead, it falls apart into three modules, corresponding to three major checkpoints that gate the G_1/S, G_2/M and M/G_1 transitions (we found no evidence for a regulatory S/G_2 boundary). Judged on the available data, these three subnetworks only interact indirectly through the progression of the DNA, ND, and CD cycles (Figure 1c). Arguably, this makes perfect sense, as the control network must be responsive to the state of the cell division cycle. At the same time, this is not widely recognised in the literature, and several current models of the cell division cycle directly link the three regulatory modules into a clock-like network. Our findings here suggest that this is incorrect.

Merging perspectives: A role for the DNA damage response in normal CDC control

The GSM connects knowledge from several distinct areas of research. When we combined knowledge from the cell cycle and DNA damage research fields, a clear picture emerged of how DNA replication is monitored and how this prevents mitotic entry. Ongoing DNA replication leads to ssDNA/Rad53 signalling from replication forks (Figure 2). This signal maintains S-phase transcription (through inhibition of the Nrm1 repressor; Fig S5), and inhibits the G_2/M transition through transcriptional inhibition of the *CLB2* cluster (through inhibition of the Ndd1 activator; Fig S7) and through post-translational inhibition of Cdc28-

Clb2 through stabilisation of the inhibitory CDK tyrosine kinase Swe1 (Fig S9). While the S-phase checkpoint is well known from studies on DNA damage and repair, its function is again not (widely) recognised in the literature on the cell division cycle control. However, the essential function of Mec1/Rad53 signalling in normal cell cycle control suggests that this may be its primary function.

Executing the logic: Ordered progression of the cell division cycle and nutrient dependent G_0 arrest

Next, we analysed the GSM through parameter-free simulation. The rxncon network is not directly executable, but compilable into a uniquely defined bBM[21]. We used the bBM to evaluate the completeness of the cell division cycle model in three steps: First, we searched for a point attractor in the absence of nutrients, reflecting G_0 arrest. Second, starting from this G_0 attractor, we released the cell cycle arrest through addition of nutrients and searched for a cyclic attractor with ordered progression through the three macroscopic cycles. Third, we interrupted the cyclic attractor by adding compounds known to halt cell cycle, i.e. pheromones, HU, LatA or NOC. The first step was to find an appropriate initial state vector for the model. The model has 2378 nodes and hence 2^{2378} ($\sim 10^{716}$) possible state vectors, precluding an exhaustive search. Instead, we used the bBM default vector[21]. Interestingly, the resulting point attractor is consistent with nutrient dependent G_0 arrest (Fig 3a). Next, we simulated the network from this initial state in the presence of nutrients, and evaluated the simulation trajectory and attractor to identify inconsistencies and gaps in the knowledge base. Most importantly, the crude time concept in the Boolean model caused significant problems, as shorter event chains are faster than longer ones even if they occur through slower reactions. To resolve this problem, we introduced a time-scale separation that made all transcriptional reactions and DNA replication slower than other reactions (such as post-translational modifications or protein-protein interactions), by requiring their input to be true for twenty consecutive time steps before firing (reflecting the longest signalling path). After introducing the time scale separation, which added 780 nodes to the bBM, the model accurately reflected the ordered progression through the three macroscopic cycles (Fig 3b), resulting in a cyclic attractor with period of 186. Finally, we examined the arrest points in response to pheromone, HU, LatA and NOC (Fig 3c), identifying and correcting one final issue in the network: The ability of Swe1 to inhibit mitotic entry in the absence of a proper bud. The changes made in

the network validation phase are summarised in Table 1.

Testing the model: Parameter-free simulation accurately predicts genotype-to-phenotype relationship for 63 out of 85 tested mutants

To examine the predictive power of the model, we analysed the predicted arrest point of *cdc* mutants with known phenotypes. We chose 85 (combinations of) deletions, point, and constitutive (over) expression mutants, and examined their cell cycle progression (cyclic attractor) or arrest (point attractor) (Table S2). We observe two types of cyclic attractors; a normal and ordered progression through all three macroscopic cycles (viability) and a partial cyclic attractor passing through DNA replication and nuclear division, but not cell division (resulting in multinucleate cells, scored here as lethality). In addition, we observed twelve distinct point attractors (at the level of macroscopic states), which correspond to G_1, S, G_2/M, M, and T arrest (Fig 4). The model correctly predicts all 43 lethal mutants, and 19 out of 42 viable mutants, but also scores 23 viable mutants as inviable. We note that the model is conservative in estimating viability, and look closer at the 23 inconsistent predictions (Table 2). Several of these mutants can be explained by implicit synthetic lethality[1]. I.e., the mutations are synthetically lethal *in vivo* with components for which key mechanisms are not known and hence not included in the model. For example, Clb3 and Clb4 are known to compensate for loss of Clb5, but the mechanisms are not known and, therefore, not included in the GSM. Hence, the GSM predicts the *clb5* mutant, implicitly corresponding to a *clb3clb4clb5* triple mutant, to be lethal[24]. Similarly, the mechanism by which Bck2 rescues *cln3* is unknown, explaining the lethality of the *cln3* (*bck2cln3*) mutant[25]. Seven of the 23 inconsistent predictions can be explained through implicit synthetic lethality, highlighting missing mechanistic knowledge. Some of the remaining mutants can be explained by strong phenotypes, which could be justified as “lethal” on a binary scale, such as the SBF-mutants (*swi4*, *swi6*, *swi6S4A* and *swi4swi6*) and *pds1*. Others, like *mbp1* and *cdh1*, which are predicted to be lethal but have no or weak reported phenotypes, likely indicate missing redundancy - again pointing to missing empirical knowledge. Taken together, the biological knowledge base uniquely defines a parameter-free model, which accurately predicts the vast majority of the mutant phenotypes that we tested - including point mutants.

[1]Synthetic lethality: The combination of two or more mutations that are individually viable results in lethality.

DISCUSSION

We present a genome-scale mechanistic model of the cell division cycle. It is mechanistic, as the connections within the model correspond to direct biochemical reactions or dependencies of these reactions on the state of the reactants, down to the level of specific residues and domains. It is genome-scale, as it accounts for all components in the cell division cycle for which we could assign a mechanistic function. We visualise the complete knowledge base as a single connected network, and show that it defines an executable model. We use this model for validation of the network and to predict genotype-to-phenotype relationships down to the resolution of specific residues.

The genome-scale scope allows us to interpret missing features. The most striking observation is the lack of a single cycle: The control network falls apart into three distinct control circuits; G_1/S, G_2/M and M/G_1, which monitor and control three distinct replication cycles: DNA replication, nuclear division and cell division. While missing connections may reflect missing knowledge, the modularity we observe seems to make perfect sense: The control network needs to be more than a sizer/timer; it must respond to the replication cycles it controls. Similarly, the replication cycles must be independent to explain ploidy shifts, multi-nucleate (or nuclei-free) cells and meiosis. Nevertheless, the regulatory mechanisms that uncouple these cycles remain largely unknown even in baker's yeast.

These findings have implications for our understanding of the CDC. The regulatory network has previously been modelled as a closed cycle, without being explicitly dependent on the progression of the replication events. For example, it has been difficult to find a mechanistic link between the G_1/S (Cln1/2, Clb5/6 expression) and G_2/M (Clb1/2 expression) transitions. We and others have modelled this as a gene expression cascade (Clb5/6 -> Clb3/4 -> Clb1/2), but without being able to explain how this cascade responds to e.g. HU-induced S-phase arrest[26,27]. By combining knowledge from two fields, we explain this through Mec1/Rad53 signalling from replication forks to both transcriptional and posttranslational inhibition of the Cdc28-Clb1/2 kinase complex. This knowledge was available in the literature but was only brought together to explain cell cycle regulation through the genome-scale perspective.

Despite its scope, the GSM we present here comes with several limitations. First, it is a biological knowledge base focussed on qualitative information. Second, this information is limited by literature data coverage and quality. Although the CDC of *S. cerevisiae* is exceptionally well known, we repeatedly had to introduce gap-filling assumptions when

knowledge is uncertain or missing. Third, the mutant analysis indicates missing redundancies and that certain effects cannot be properly described at the qualitative level only. Fourth, the model does not explicitly include spatial aspects, as complex level properties (such as localisation) cannot currently be expressed in the rxncon language. Fifth and finally, the Boolean modelling logic is a very crude approximation both quantitatively and temporally, and we needed to introduce time-scale separation between transcription and the other signalling events. Quantitative models will be required to analyse processes such as dynamics of cell structures or polarity establishment. However, it is currently not possible to build a quantitative model at this scale, as it would require thousands of undefined parameters values. As for metabolic networks[2], the qualitative information is more abundant and less uncertain, and qualitative models can capture the vast majority of the mutant phenotypes. Interestingly, the discrepancies between model predictions and known phenotypes primarily identified missing redundancies, i.e. missing empirical knowledge, rather than methodological limitations. Hence, this first GSM draft highlights the need for further dedicated work on the experimental characterisation of this fundamental model system.

This work is complementary to quantitative modelling efforts. While we can read out 1403 variables - elemental reactions and states - their values are limited to True or False. In contrast, quantitative models can precisely predict quantitative or complex phenotypes, such as cell cycle duration, cell size distribution, and polarity establishment[17,19,28]. However, the presented model is much larger in scope than these quantitative models, and only the Kaizu map is similar in scope although not executable[20]. One of the major outstanding challenges will be to reconcile the two: Genome-scale scope and quantitative modelling. While our model could in principle be converted into an RBM[22], a number of hurdles remain: First, there is no clear equivalence to rxncon inputs in RBMs and the connections between modules would need to be hand-crafted. Second, we would need to find or estimate values for >790 unique parameters. Third, we would need representations of the DNA replication, nuclear division, and cell division cycles that are compatible with agent-based simulation. In the foreseeable future, meaningful simulation of signal transduction networks at this scale will most likely remain qualitative or semi-quantitative, as it does for metabolic networks.

Here, we show that it is possible to build, visualise and simulate mechanistic genome-scale models of eukaryotic signal transduction networks. Until today, this has only been done for metabolic networks, and the mass-transfer logic leads to crippling scalability issues when applied to signal transduction networks (due to microstate enumeration; reviewed in: 5,6,12). We solve this technical issue by using a formalism with adaptive resolution. We chose rxncon, as it is text-based rather than graphical, uses a higher-level biological language rather than model code, supports scalable visualisation, and is compilable into a parameter-free model for direct simulation[21,29]. In particular, we find the iterative visualisation in the regulatory graph invaluable in the model construction process, and present the final model in a wall-chart that is inspired by the biochemical pathway maps[30]. In addition, the ability to go from a pure biological knowledge base to a parameter-free model that can predict system level features from molecular mechanisms is highly non-trivial[5]. Here, we use this feature for network validation - by iteratively analysing and improving the network until the corresponding model reproduces wild-type behaviour - and for genotype-to-phenotype predictions of 85 mutants. Hence, we bring together the mechanistic precision in the molecular biology, the scope of the comprehensive maps, and the executability of the mathematical models. A similar high-resolution knowledge base on the information processing network in human cells would be an important step towards a human whole-cell model and - when it accounts for the molecular effect of allele differences and drug perturbations - truly personalised medicine.

FIGURE LEGENDS

Figure 1: The molecular architecture of the CDC control network. (a) The model consists of seven parts: (i) Gene expression, (ii) regulated degradation, (iii) CDK assembly and activation, (iv) DNA replication, (v) SPB duplication and nuclear division, (vi) cell division, and (vii) a set of reactions involving cell cycle components but without (known) regulatory connections to the main network. The outputs of the mechanistic reaction network (MRN) in modules (iv)-(vi) determine the progression of the coarse-grained model (CGM). **(b)** The CGM consists of three parts: (left) SPB duplication and nuclear division, (middle) DNA replication, and (right) Cell division. The MRN and CGM parts communicate via an input/output layer. (c) Schematic representation of the network architecture. The three independent replication cycles are regulated by three disjunct control modules gating the G_1/S, G_2/M and M/G_1 transitions. At mitotic exit, the combined activity of Cdc14 and APC/C resets the state of the cell cycle network. (d) The difference between microstate (-reactions) and elemental states and reactions. Elemental state variables (residues and domains) can be thought of as dimensions, and each elemental state as defined in only one dimension. In contrast, microstates are fully defined positions in this state space. Hence, there is a one-to-many relationship between elemental states and microstates, as several of the latter match one of the former. The discrepancy between the two increases with the number of elemental state variables and hence dimensions. Similarly, an elemental reaction would denote all transitions along a single axis, which can correspond to multiple microstate reactions depending on reaction context. In a rxncon model, the latter is captured by contingencies. E.g., in this case, T169 phosphorylation is a prerequisite for cyclin binding, limiting the possible reaction trajectory to a single path.

Figure 2: The Mec1/Rad53 pathway senses ongoing DNA replication to inhibit mitotic entry. Ongoing DNA replication leads to exposed ssDNA and ssDNA/dsDNA junctions at the replication forks, which are sensed by the Mec1/Rad53 pathway. Mec1 phosphorylates and stabilises Swe1, a Cdk1-Clb1/2 inhibitor, and Rad53 phosphorylates and inhibits Nrm1, an inhibitor of the MBF transcription factor, and Ndd1, which is needed for *CLB1/2* transcription. The regulatory graph is a bipartite representation where elemental reactions (red) produce or consume elemental states (blue), and elemental states influence - through contingencies - elemental reactions. Complex contingencies are collected in Boolean nodes

(AND/OR/NOT; light grey), and Input/Output nodes (dark grey) define the interface between the model and its surroundings - and between the MRN and CGM parts.

Figure 3: The parameter-free model reproduces both cell cycle progression and arrest. Simulation results visualised on the CGM states, the cyclins Cln3, Cln2 and Clb5, the active form of the CDKI Sic1, and three selected elemental states: Mec1 phosphorylated Rad53 (indicative of ongoing DNA replication), Tyr19 phosphorylated Cdc28 (inhibition of Cdc28-Clb1/2) and Cdc28 not bound to Far1 (disappears during pheromone arrest). (a) When the model is simulated with nutrients set to False, the cells arrest at G_0: With licensed DNA, SPB-satellite, without bud and without cyclin or Rad53 activity. (b) When cells are released from the G_0 arrest by setting nutrients to True, they progress through the cell division cycle by replicating their DNA, undergoing nuclear division and rapidly thereafter cell division, and resetting the network for a new division, traversing 186 Boolean steps. Cyclin activities rise and fall through cyclin expression and inhibition by Sic1 and Swe1 (Tyr19 kinase). (c) The cells arrest again when exposed to pheromone (G_1: licensed DNA, SPB-satellite, no bud, only Cln3 present), HU (S: replicating DNA, duplicated SPB, large bud, Cdc28-Cln2, Cdc28-Clb5 and Rad53 are active), LatA (G_2/M: replicated DNA, duplicated SPB, small bud, only Cdc28-Cln2 active) and NOC (M: replicated DNA, duplicated SPB, large bud, and high Cdc28-Clb2 activity (not shown)).

Figure 4: The model predicts the phenotypes of a majority of all tested mutants. Simulations were performed by introducing deletions (setting all protein states (and mRNA and Gene, if appropriate) to False), point mutations (by locking proteins in a certain modification state) or constitutive overexpression (by setting the transcription reaction to True constantly), and the mutants were analysed through simulation by release from the (modified) G_0 state of the wild-type. (a) The model predicts the correct phenotype (dead or alive) for 62 out of 85 mutants, although closer inspection revealed that several of the 23 inconsistent mutants can be explained by implicit synthetic lethality or strong phenotypes (Table 2). (b) The 62 mutants that are predicted to be dead arrest at thirteen distinct arrest points, that correspond to G_1 (1a-c, 5*, 6*), S (2), G_2/M (3a-e), M (4) and T (5*, 6*) arrest, or progress through a partial cyclic attractor with repeated DNA replication and nuclear division but no cell division, resulting in multinucleate cells. Note that group 5 and 6 contains G_1 and T

arrested cells that completed nuclear division but arrest before cytokinesis. They can only be distinguished on the DNA/Nuclei count (Table S3).

Table 1: List of gap-filling additions. The table summarises the gap-filling changes made to the network in order to fully connect the regulatory logic and to reproduce wild type behaviour: G0 arrest in the absence of nutrients, ordered progression through all three macroscopic cycles in the CGM in the presence of nutrients, and proper cell cycle arrest in response to pheromone, HU, LatA and NOC. Some of these changes are supported by non-conclusive literature evidence, some are technical modifications only included to allow meaningful bBM simulation (e.g. the time delays), and some constitute testable hypotheses. Specific additions and changes are indicated in Table S1.

Table 2: List of mutants with phenotypic predictions that are inconsistent with observed phenotypes. The model predicted 23 viable mutants to be lethal. Of these, seven mutants can be explained by implicit synthetic lethality: While *cln3* and *clb5* are viable, the model lacks implementation of mechanistic functions of Bck2 and Clb3/Clb4, which are necessary in the absence of Cln3 and Clb5, respectively. While other mutants have strong phenotypes in e.g. cell size or growth rate, such as *swi4*, *swi6* and *pds1*, others - like *cdh1* - have no strong phenotypes as single mutations, suggesting that redundancy mechanisms are missing in our current knowledge.

Supplementary Material: Model description. Detailed description of the biology and implementation of the cell division cycle network.

Fig S1: The molecular architecture of the cell division cycle. Poster sized version of the network map displayed in Fig 1A. Also available at https://github.com/rxncon/models/ as CDC_S_cerevisiae_poster.pdf.

Table S1: The rxncon model. The rxncon network definition consists of four sheets: (i) A reaction list defining all elemental reactions - and implicitly all elemental states - of both the CGM and the MRN, (ii) a contingency list defining the contextual constraints on the elemental reactions, (iii) a reaction definition which gives the semantic meaning of all elemental reactions, and (iv) a modification definition which lists all valid modifiers. The structure and use of the rxncon model file is described in detail elsewhere[22,29]. The GSM is also available at https://github.com/rxncon/models/ as CDC_S_cerevisiae.xls.

Table S2: Supplementary references. A list of all references used to construct the model.

Table S3: List of mutants examined in this study. This table lists the 85 mutants used to test the model and indicate the phenotype (viable/lethal) as well as point of arrest and the DNA copy number and number of nuclei at arrest.

Sup File 1: Cytoscape file. The cytoscape file containing the regulatory graph of the complete network as well as of the individual modules presented in the supplementary figures.

Sup File 2-4: Boolean model, initial vector, label key. These three files where used to simulate the network model, as described in detail elsewhere[21]. File S2 contains the model code, formatted for simulation using BoolNet. File S3 contains the initial vector. File S4 defines the mapping between the short names used in files S2 and S3 to the names used in the rxncon file.

ACKNOWLEDGEMENTS

The authors would like to thank Jesper Romers, Sebastian Thieme and Mathias Wajnberg for close collaboration in the methods development, and Matteo Barberis for critical comments on the network model. MK would like to thank Hiroaki Kitano and Stefan Hohmann for the inspiration and support to tackle the challenge of large-scale signalling networks. This work was supported by the German Federal Ministry of Education and Research via e:Bio Cellemental (FKZ0316193, to MK).

ONLINE METHODS

The cell division cycle model was created using the second generation rxncon language[29], using an iterative workflow described in detail elsewhere[22]. The rxncon model consists of two types of statements that both correspond directly to empirical data. First, *elemental reactions* define decontextualised reaction events in terms of changes in elemental states. An elemental reaction is essentially a reaction centre in a RBM[31]. Second, *contingencies* define constraints on the elemental reactions in terms of (Boolean combinations of) elemental states.

Elemental reactions can be either mono- or bimolecular, but always defined through two components; A and B, which are the same in monomolecular reactions. Each component is defined at a certain resolution, depending on the reaction type and the component's role in that reaction (see 29 for details). Elemental reactions contain no contextual information beyond the state that changes: E.g., a phosphorylation reaction requires that the target residue is unphosphorylated. Any additional context is defined as contingencies.

Contingencies define which states (or inputs) must be true or false for an elemental reaction to take place. The rxncon language only considers direct mechanistic effects, i.e. the states must belong either to the reactants or to a complex the reactants are part of. In the latter case, complexes are defined through structured Boolean contingencies (see 29 for details).

The complete set of contingencies for a single elemental reaction defines the reaction context(s) in a RBM, but in rxncon the context definition is separated over several contingencies that each define the impact of a single elemental state[29]. This gives a one-to-one correspondence between model definition and empirical data, improving composability as model changes and extension have a local impact only. Multiple contingencies can be combined into statements that are arbitrarily complex, defining reactions down to microstate resolution when necessary. Typically, however, single or few contingencies per elemental reaction suffice to capture all the empirically known regulatory mechanisms. In the end, the rxncon model constitutes a molecular biology knowledge base in formal language, which is computer readable, can be automatically visualised and compiled into a uniquely defined executable model.

For a detailed description of how to build a rxncon model, see 22.

Parameter-free models were created automatically using the rxncon compiler[21], and simulated with the R package BoolNet[32]. The rxncon software can be downloaded from https://github.com/rxncon/rxncon or directly installed from the python package index ("pip install rxncon"). See https://rxncon.org for further instructions.

The initial G_0 simulation was performed with the default vector, except that the placeholder input [Histones] was set to true. This simulation resulted in a point attractor considered to correspond to G_0 arrest in the absence of nutrients. The following simulations were performed from this starting state with nutrients set to true only (for normal cell cycle progression), or in combination with either chemical inputs (Pheromone, HU, LatA or NOC) set to True or with changes reflecting the mutations (all states of deleted components and their genes/mRNA when applicable) set to False; phosphorylated/unphosphorylated states set to constant True/False for Alanine or phosphomimetic residue changes; transcription set to constant True for (constant) over expression). The final attractor and path to attractor were analysed for each condition to determine phenotypes and arrest point.

The cell division cycle model was visualised as rxncon regulatory graphs[10], using Cytoscape (http://www.cytoscape.org/) and a visual formatting file (rxncon2cytoscape.xml; https://github.com/rxncon/tools).

The cell division cycle model is compiled in an SBtab compatible spreadsheet[33], and is available in Table S1 and from https://github.com/rxncon/models (CDC_S_cerevisiae.xls). The model is fully referenced through the "reference" columns in the reaction and contingency sheet, and explained in detail in the supplementary material.

The model is based on the literature listed in Table S3, as specified for individual reactions and contingencies in Table S1.

REFERENCES

1 Kitano, H. Computational systems biology. *Nature* **420**, 206-210, doi:10.1038/nature01254 (2002).

2 Herrgard, M. J. *et al.* A consensus yeast metabolic network reconstruction obtained from a community approach to systems biology. *Nat Biotechnol* **26**, 1155-1160, doi:10.1038/nbt1492 (2008).

3 Thiele, I. *et al.* A community-driven global reconstruction of human metabolism. *Nat Biotechnol* **31**, 419-425, doi:10.1038/nbt.2488 (2013).

4 Karr, J. R. *et al.* A whole-cell computational model predicts phenotype from genotype. *Cell* **150**, 389-401, doi:10.1016/j.cell.2012.05.044 (2012).

5 Hlavacek, W. S. & Faeder, J. R. The complexity of cell signaling and the need for a new mechanics. *Sci Signal* **2**, pe46, doi:10.1126/scisignal.281pe46 (2009).

6 Münzner, U., Lubitz, T., Klipp, E. & Krantz, M. in *Systems Biology* (eds J. Nielsen & S. Hohmann) 215-242 (Wiley, 2017).

7 Blinov, M. L., Faeder, J. R., Goldstein, B. & Hlavacek, W. S. BioNetGen: software for rule-based modeling of signal transduction based on the interactions of molecular domains. *Bioinformatics* **20**, 3289-3291, doi:10.1093/bioinformatics/bth378 (2004).

8 Danos, V., Feret, J., Fontana, W., Harmer, R. & Krivine, J. in *CONCUR 2007 – Concurrency Theory: 18th International Conference, CONCUR 2007, Lisbon, Portugal, September 3-8, 2007. Proceedings* (eds Luís Caires & Vasco T. Vasconcelos) 17-41 (Springer Berlin Heidelberg, 2007).

9 Le Novere, N. *et al.* The Systems Biology Graphical Notation. *Nat Biotechnol* **27**, 735-741, doi:10.1038/nbt.1558 (2009).

10 Tiger, C. F. *et al.* A framework for mapping, visualisation and automatic model creation of signal-transduction networks. *Mol Syst Biol* **8**, 578, doi:10.1038/msb.2012.12 (2012).

11 Rother, M., Münzner, U., Thieme, S. & Krantz, M. Information content and scalability in signal transduction network reconstruction formats. *Mol Biosyst* **9**, 1993-2004, doi:10.1039/c3mb00005b (2013).

12 Chylek, L. A., Harris, L. A., Faeder, J. R. & Hlavacek, W. S. Modeling for (physical) biologists: an introduction to the rule-based approach. *Phys Biol* **12**, 045007, doi:10.1088/1478-3975/12/4/045007 (2015).

13 Enserink, J. M. & Kolodner, R. D. An overview of Cdk1-controlled targets and

processes. *Cell Div* **5**, 11, doi:10.1186/1747-1028-5-11 (2010).

14 Howell, A. S. & Lew, D. J. Morphogenesis and the cell cycle. *Genetics* **190**, 51-77, doi:10.1534/genetics.111.128314 (2012).

15 Hartwell, L. H., Culotti, J. & Reid, B. Genetic control of the cell-division cycle in yeast. I. Detection of mutants. *Proc Natl Acad Sci U S A* **66**, 352-359 (1970).

16 Goldbeter, A. A minimal cascade model for the mitotic oscillator involving cyclin and cdc2 kinase. *Proc Natl Acad Sci U S A* **88**, 9107-9111 (1991).

17 Chen, K. C. *et al.* Kinetic analysis of a molecular model of the budding yeast cell cycle. *Mol Biol Cell* **11**, 369-391 (2000).

18 Chasapi, A. *et al.* An Extended, Boolean Model of the Septation Initiation Network in S.Pombe Provides Insights into Its Regulation. *PloS one* **10**, e0134214, doi:10.1371/journal.pone.0134214 (2015).

19 Kraikivski, P., Chen, K. C., Laomettachit, T., Murali, T. M. & Tyson, J. J. From START to FINISH: computational analysis of cell cycle control in budding yeast. *NPJ Syst Biol Appl* **1**, 15016, doi:10.1038/npjsba.2015.16 (2015).

20 Kaizu, K. *et al.* A comprehensive molecular interaction map of the budding yeast cell cycle. *Mol Syst Biol* **6**, 415, doi:10.1038/msb.2010.73 (2010).

21 Romers, J. C., Thieme, S., Münzner, U. & Krantz, M. Pre-print: A scalable method for parameter-free simulation and validation of mechanistic cellular signal transduction network models. *bioRxiv* (2017).

22 Romers, J., Thieme, S., Münzner, U. & Krantz, M. in *Modeling Biomolecular Site Dynamics Methods in Molecular Biology* (ed W. S. Hlavacek) (Springer, 2018).

23 Neiman, A. M. Sporulation in the budding yeast Saccharomyces cerevisiae. *Genetics* **189**, 737-765, doi:10.1534/genetics.111.127126 (2011).

24 Schwob, E. & Nasmyth, K. CLB5 and CLB6, a new pair of B cyclins involved in DNA replication in Saccharomyces cerevisiae. *Genes Dev* **7**, 1160-1175 (1993).

25 Epstein, C. B. & Cross, F. R. Genes that can bypass the CLN requirement for Saccharomyces cerevisiae cell cycle START. *Mol Cell Biol* **14**, 2041-2047 (1994).

26 Linke, C. *et al.* A Clb/Cdk1-mediated regulation of Fkh2 synchronizes CLB expression in the budding yeast cell cycle. *NPJ Syst Biol Appl* **3**, 7, doi:10.1038/s41540-017-0008-1 (2017).

27 Spiesser, T. W. *et al.* A yeast cell cycle model integrating stress, signaling, and physiology. (Submitted).

28 Giese, W., Eigel, M., Westerheide, S., Engwer, C. & Klipp, E. Influence of cell shape,

inhomogeneities and diffusion barriers in cell polarization models. *Phys Biol* **12**, 066014, doi:10.1088/1478-3975/12/6/066014 (2015).

29 Romers, J. C. & Krantz, M. Pre-print: rxncon 2.0: a language for executable molecular systems biology. *bioRxiv*, doi:10.1101/107136 (2017).

30 Michal, G. Roche Biochemical Pathways (wall chart). (2014).

31 Faeder, J. R., Blinov, M. L. & Hlavacek, W. S. Rule-based modeling of biochemical systems with BioNetGen. *Methods in molecular biology (Clifton, N.J.)* **500**, 113-167, doi:10.1007/978-1-59745-525-1_5 (2009).

32 Mussel, C., Hopfensitz, M. & Kestler, H. A. BoolNet--an R package for generation, reconstruction and analysis of Boolean networks. *Bioinformatics* **26**, 1378-1380, doi:10.1093/bioinformatics/btq124 (2010).

33 Lubitz, T. *et al.* SBtab: a flexible table format for data exchange in systems biology. *Bioinformatics*, doi:10.1093/bioinformatics/btw179 (2016).

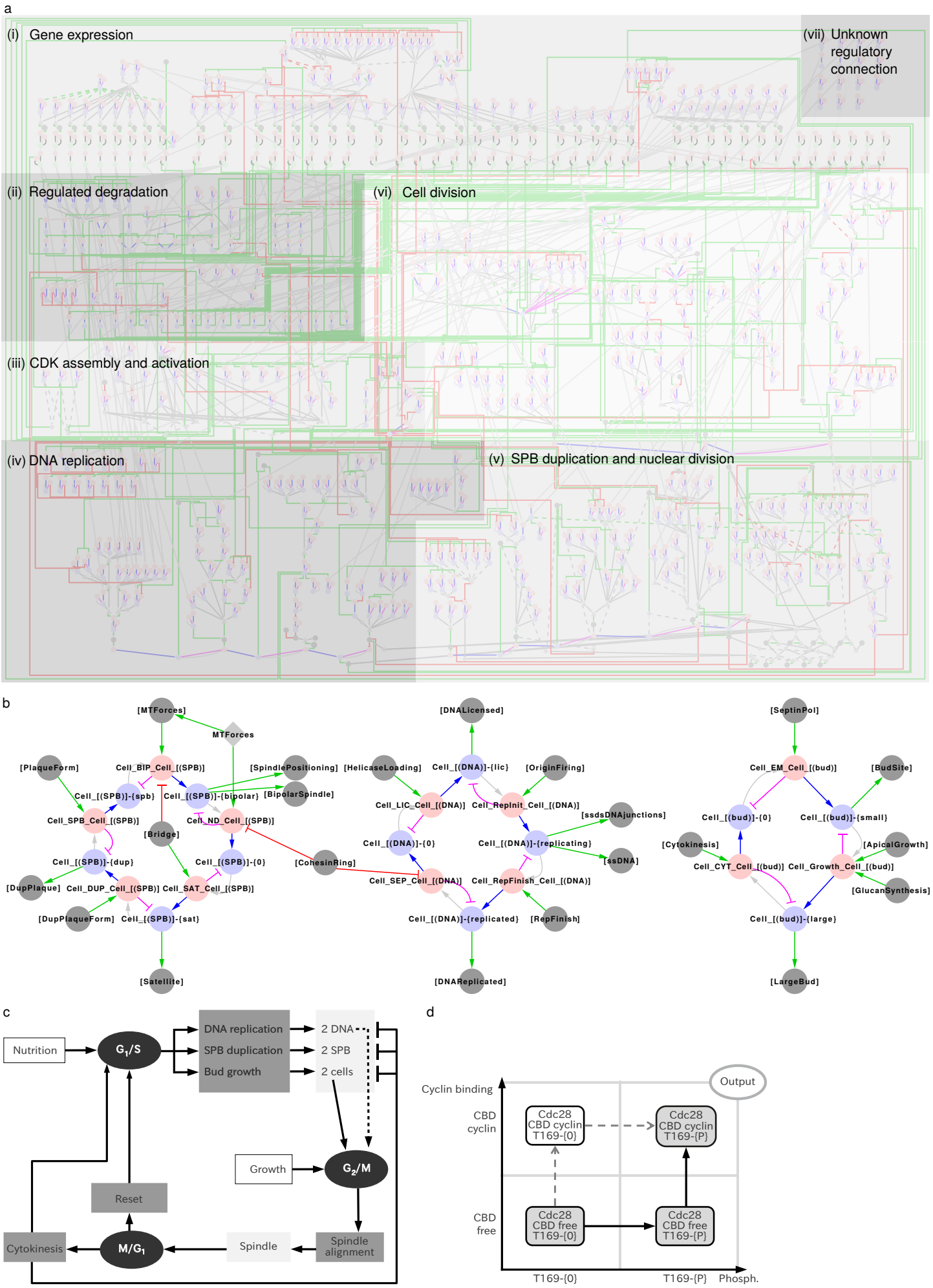
a
(i) Gene expression
(vii) Unknown regulatory connection
(ii) Regulated degradation
(vi) Cell division
(iii) CDK assembly and activation
(iv) DNA replication
(v) SPB duplication and nuclear division
b
[MTForces]
MTForces
[PlaqueForm]
Cell_BIP_Cell_[(SPB)]
[SpindlePositioning]
[HelicaseLoading]
Cell_[(DNA)]-{lic}
[OriginFiring]
[DNALicensed]
[SeptinPol]
Cell_EM_Cell_[(bud)]
[BudSite]
Cell_[(SPB)]-{spb}
Cell_[(SPB)]-{bipolar}
[BipolarSpindle]
Cell_LIC_Cell_[(DNA)]
Cell_ReplInit_Cell_[(DNA)]
[ssdsDNAjunctions]
Cell_[(bud)]-{0}
Cell_[(bud)]-{small}
Cell_SPB_Cell_[(SPB)]
Cell_ND_Cell_[(SPB)]
[Bridge]
Cell_[(DNA)]-{0}
Cell_[(DNA)]-{replicating}
[ssDNA]
[Cytokinesis]
[ApicalGrowth]
Cell_[(SPB)]-{dup}
Cell_[(SPB)]-{0}
[CohesinRing]
Cell_SEP_Cell_[(DNA)]
Cell_RepFinish_Cell_[(DNA)]
Cell_CYT_Cell_[(bud)]
Cell_Growth_Cell_[(bud)]
[GlucanSynthesis]
[DupPlaque]
Cell_DUP_Cell_[(SPB)]
Cell_SAT_Cell_[(SPB)]
[DupPlaqueForm]
Cell_[(SPB)]-{sat}
Cell_[(DNA)]-{replicated}
[RepFinish]
Cell_[(bud)]-{large}
[Satellite]
[DNAReplicated]
[LargeBud]
c
Nutrition
G1/S
DNA replication
SPB duplication
Bud growth
2 DNA
2 SPB
2 cells
Growth
G2/M
Reset
Cytokinesis
M/G1
Spindle
Spindle alignment
d
Output
Cyclin binding
CBD cyclin
CBD free
Cdc28 CBD cyclin T169-{0}
Cdc28 CBD cyclin T169-{P}
Cdc28 CBD free T169-{0}
Cdc28 CBD free T169-{P}
T169-{0}
T169-{P}
Phosph.

Figure 1

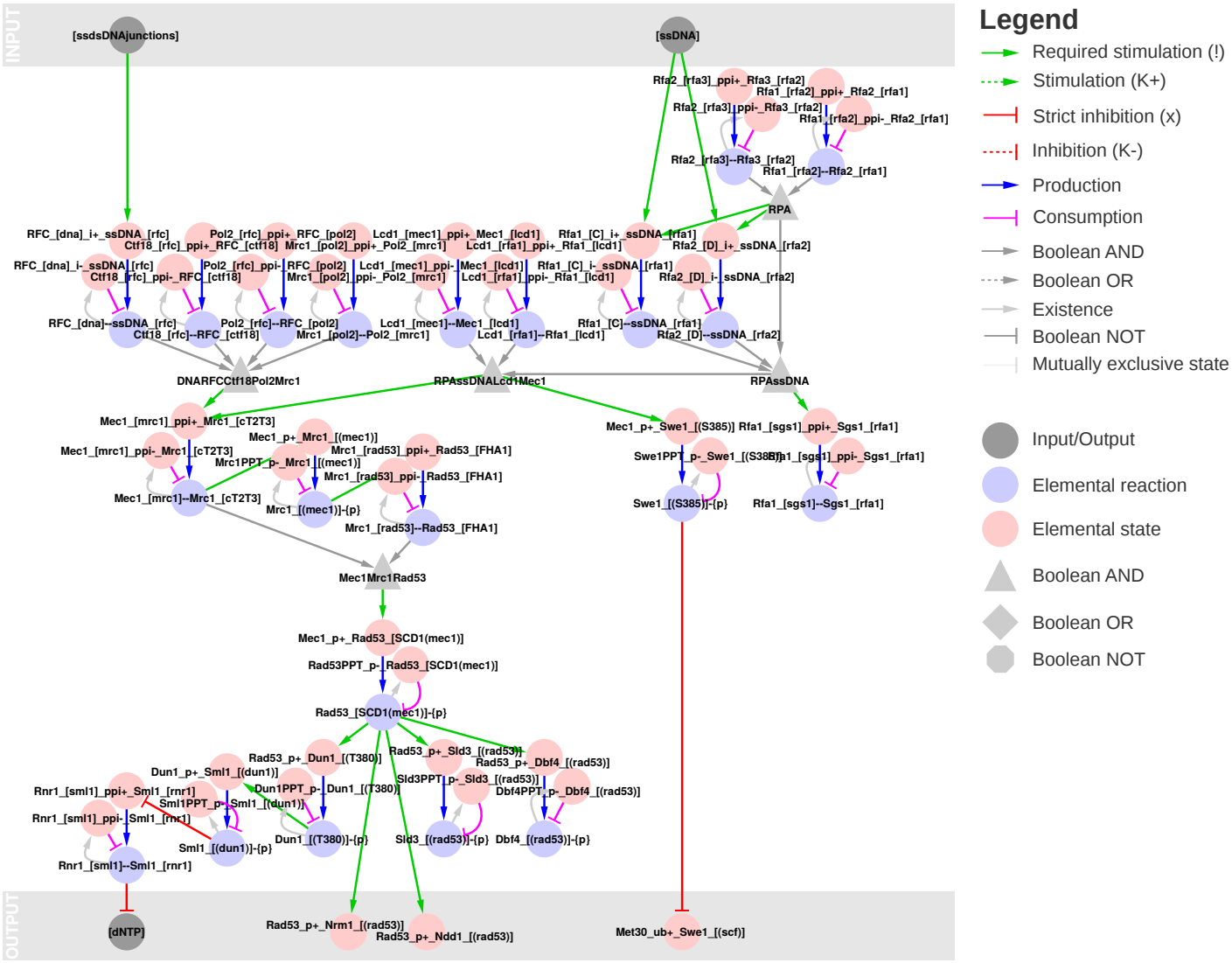
INPUT
[ssdsDNAjunctions]
[ssDNA]
Rfa2_[rfa3]_ppi+_Rfa3_[rfa2]
Rfa1_[rfa2]_ppi+_Rfa2_[rfa1]
Rfa2_[rfa3]_ppi-_Rfa3_[rfa2]
Rfa1_[rfa2]_ppi-_Rfa2_[rfa1]
Rfa2_[rfa3]--Rfa3_[rfa2]
Rfa1_[rfa2]--Rfa2_[rfa1]
RPA
RFC_[dna]_i+_ssDNA_[rfc]
Ctf18_[rfc]_ppi+_RFC_[ctf18]
Pol2_[rfc]_ppi+_RFC_[pol2]
Mrc1_[pol2]_ppi+_Pol2_[mrc1]
Lcd1_[mec1]_ppi+_Mec1_[lcd1]
Lcd1_[rfa1]_ppi+_Rfa1_[lcd1]
Rfa1_[C]_i+_ssDNA_[rfa1]
Rfa2_[D]_i+_ssDNA_[rfa2]
RFC_[dna]_i-_ssDNA_[rfc]
Ctf18_[rfc]_ppi-_RFC_[ctf18]
Pol2_[rfc]_ppi-_RFC_[pol2]
Mrc1_[pol2]_ppi-_Pol2_[mrc1]
Lcd1_[mec1]_ppi-_Mec1_[lcd1]
Lcd1_[rfa1]_ppi-_Rfa1_[lcd1]
Rfa1_[C]_i-_ssDNA_[rfa1]
Rfa2_[D]_i-_ssDNA_[rfa2]
RFC_[dna]--ssDNA_[rfc]
Ctf18_[rfc]--RFC_[ctf18]
Pol2_[rfc]--RFC_[pol2]
Mrc1_[pol2]--Pol2_[mrc1]
Lcd1_[mec1]--Mec1_[lcd1]
Lcd1_[rfa1]--Rfa1_[lcd1]
Rfa1_[C]--ssDNA_[rfa1]
Rfa2_[D]--ssDNA_[rfa2]
DNARFCCtf18Pol2Mrc1
RPAssDNALcd1Mec1
RPAssDNA
Mec1_[mrc1]_ppi+_Mrc1_[cT2T3]
Mec1_p+_Mrc1_[(mec1)]
Mec1_[mrc1]_ppi-_Mrc1_[cT2T3]
Mrc1_[rad53]_ppi+_Rad53_[FHA1]
Mrc1PPT_p-_Mrc1_[(mec1)]
Mrc1_[rad53]_ppi-_Rad53_[FHA1]
Mec1_[mrc1]--Mrc1_[cT2T3]
Mrc1_[(mec1)]-{p}
Mrc1_[rad53]--Rad53_[FHA1]
Mec1_p+_Swe1_[(S385)]
Rfa1_[sgs1]_ppi+_Sgs1_[rfa1]
Swe1PPT_p-_Swe1_[(S385)]
Rfa1_[sgs1]_ppi-_Sgs1_[rfa1]
Swe1_[(S385)]-{p}
Rfa1_[sgs1]--Sgs1_[rfa1]
Mec1Mrc1Rad53
Mec1_p+_Rad53_[SCD1(mec1)]
Rad53PPT_p-_Rad53_[SCD1(mec1)]
Rad53_[SCD1(mec1)]-{p}
Rad53_p+_Dun1_[(T380)]
Rad53_p+_Sld3_[(rad53)]
Rad53_p+_Dbf4_[(rad53)]
Dun1_p+_Sml1_[(dun1)]
Dun1PPT_p-_Dun1_[(T380)]
Sld3PPT_p-_Sld3_[(rad53)]
Dbf4PPT_p-_Dbf4_[(rad53)]
Rnr1_[sml1]_ppi+_Sml1_[rnr1]
Sml1PPT_p-_Sml1_[(dun1)]
Rnr1_[sml1]_ppi-_Sml1_[rnr1]
Dun1_[(T380)]-{p}
Sld3_[(rad53)]-{p}
Dbf4_[(rad53)]-{p}
Sml1_[(dun1)]-{p}
Rnr1_[sml1]--Sml1_[rnr1]
OUTPUT
[dNTP]
Rad53_p+_Nrm1_[(rad53)]
Rad53_p+_Ndd1_[(rad53)]
Met30_ub+_Swe1_[(scf)]
Legend
Required stimulation (!)
Stimulation (K+)
Strict inhibition (x)
Inhibition (K-)
Production
Consumption
Boolean AND
Boolean OR
Existence
Boolean NOT
Mutually exclusive state
Input/Output
Elemental reaction
Elemental state
Boolean AND
Boolean OR
Boolean NOT

Figure 2

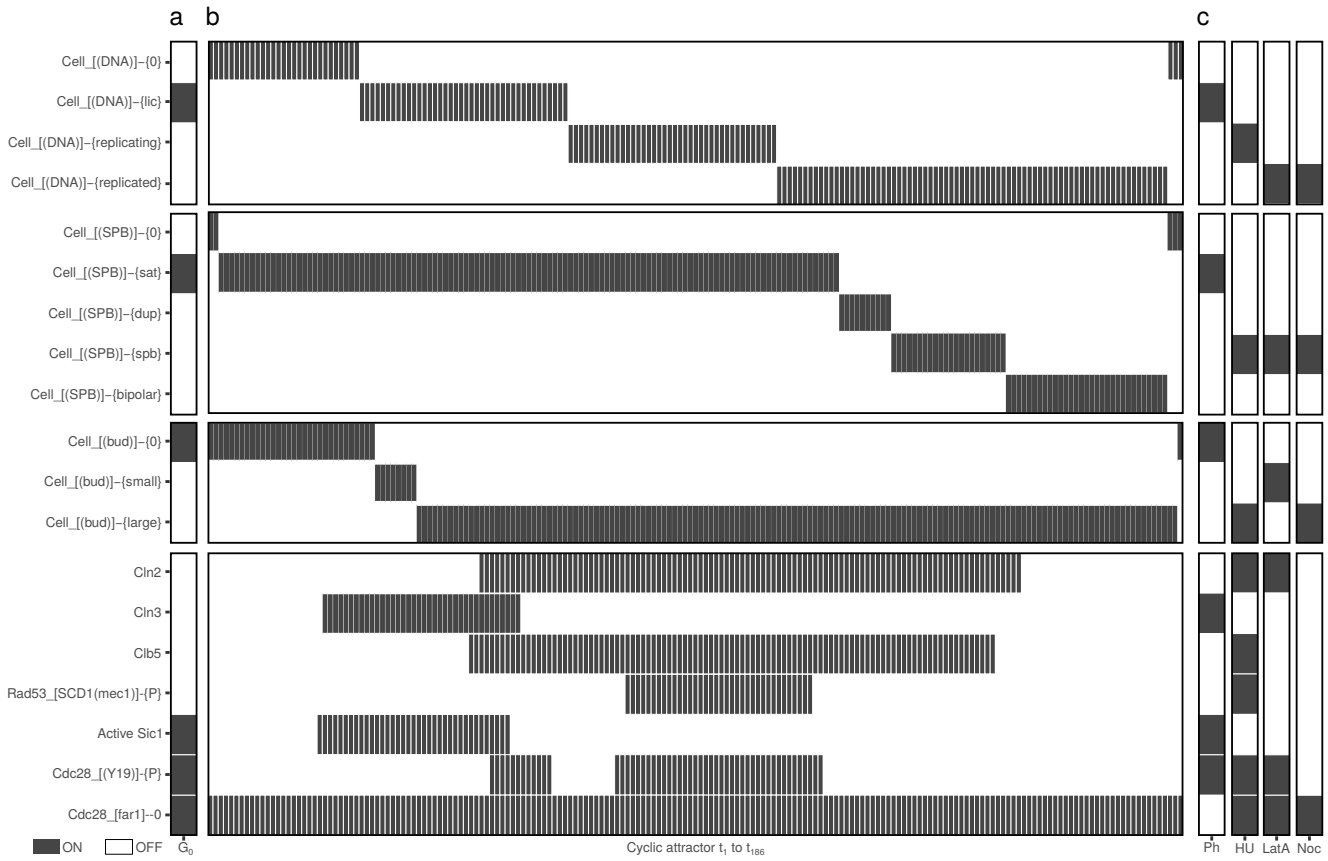
a
b
c
Cell_[(DNA)]–{0}
Cell_[(DNA)]–{lic}
Cell_[(DNA)]–{replicating}
Cell_[(DNA)]–{replicated}
Cell_[(SPB)]–{0}
Cell_[(SPB)]–{sat}
Cell_[(SPB)]–{dup}
Cell_[(SPB)]–{spb}
Cell_[(SPB)]–{bipolar}
Cell_[(bud)]–{0}
Cell_[(bud)]–{small}
Cell_[(bud)]–{large}
Cln2
Cln3
Clb5
Rad53_[SCD1(mec1)]-{P}
Active Sic1
Cdc28_[(Y19)]-{P}
Cdc28_[far1]--0
ON
OFF
G0
Cyclic attractor t1 to t186
Ph
HU
LatA
Noc

Figure 3

a

	Lethal	Viable
Cyclic	0	19
Point	43	23

b

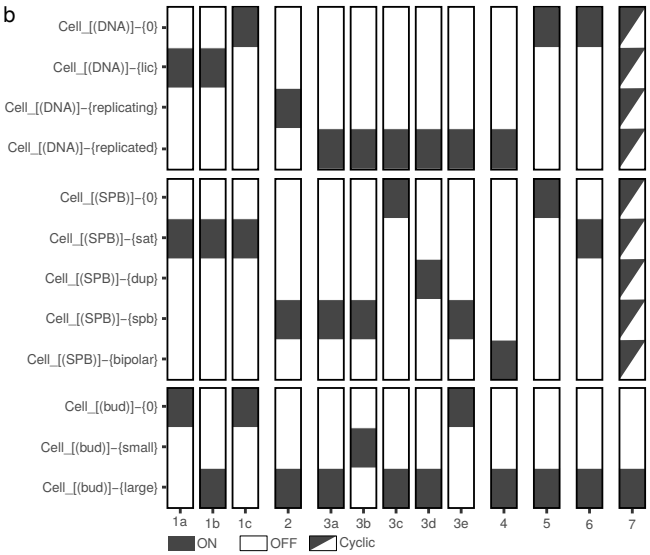

Figure 4

TABLE 1

Observation	Solution	Reference
MBF target genes constitutively expressed	Swi6 phosphorylation strict requirement for MBF activity	Palumbo et al. (2016)
Fkh2, Ndd1, Mcm1 target genes constitutively expressed	Fkh2 phosphorylation strict requirement for Fkh2 activity	Pic-Taylor et al. (2004)
Clb2 and Clb5 not degraded in G1	Ubiqitylation by both APC-Cdc20 and APC-Cdh1	Wäsch and Cross (2002), Lu et al. (2014)
Pcl9 degradation not regulated	Regulated degradation equivalent to Pcl1,2 degradation	Hernandez-Ortega et al. (2013)
Pho85-Pcl9 phosphorylation of Whi5 dominates Cdc28-mediated Whi5 phosphorylation	Pho85-Pcl9 phosphorylation positive influence on Whi5 dissociation	*Hypothesis: Alternatively, Pcl9 expression could be nutrient dependent as for Cln3*
Sic1 deactivation premature	Phosphorylation restricted to Cdc28-Cln1,2	*Hypothesis: No Cdc28-Cln3 phosphosylation of Sic1*
Bud growth module regulation insufficient	Symmetry breaking included as output/input when criteria for polarisation are fulfilled	*Placeholder for quantitative phenomenon. Cannot be described mechanstically with Boolean logic*
Stable complexes in SPB cycle disappeared	[Daughter SPB] present with duplicated and/or separated SPBs	*Technical correction*
Periodic Rad53 transcription and constant degradation lead to Rad53 periodic depletion	Constant Rad53 expression: MBF regulation as positive influence instead of strict requirement	*Hypothesis: Basal Rad53 expression constitutive to account for constant role in DNA damage response*
Discrepancy between Boolean and physiological time	Introduction of delays on transcriptional reactions	*Time scale separation. Solution to technical issue with Boolean networks.*
Dbf2 release premature	Correct spindle positioning blocks phosphorylation of Kin4 by Elm1	Consistent with SPOC activation of phosphorylation; Kurtulmus et al. 2010
No SPB duplication due to premature Spc42 disappearance. MBF transcription very brief.	Introduction of delays on replication	*Time scale separation. Solution to technical issue with Boolean networks.*
SPB positioning premature	Kar9 phosphorylation by Cdc28-Clb1,2,5,6	*Hypothesis*
No (morphological) cell division cycle due to premature activation of APC (due to Mad2 depeletion).	Degradation of Cdc20 block when bound to Mad2	*Hypothesis*
No (morphological) cell division cycle: Cytokinesis doesn't trigger as symmetry breaking and Chs2 release never overlap	Acm1 phosphorylation completely blocks (x) instead of decreases (k-) Acm1 degradation	*Hypothesis*

TABLE 2

Mutant	Arrest point	DNA	Nuclei	Comment	Synthetic Lethality
cln3	lic, sat, 0	1	1	G1-arrest	*cln3bck2*
cln3mbp1	lic, sat, 0	1	1	G1-arrest	*cln3bck2*
cln3swi6	lic, sat, 0	1	1	G1-arrest	*cln3bck2*
cln3swi4	lic, sat, 0	1	1	G1-arrest	*cln3bck2*
swi4	lic, sat, large	1	1	G1-arrest	
swi6	lic, sat, large	1	1	G1-arrest	
swi64A	lic, sat, large	1	1	G1-arrest	
mbp1	lic, sat, large	1	1	G1-arrest	
clb5	lic, sat, large	1	1	G1-arrest	*clb3clb4clb5*
cdc20pds1clb5	lic, sat, large	1	1	G1-arrest	*clb3clb4clb5*
cdc20pds1clb5cdh1SIC1	lic, sat, large	1	1	G1-arrest	*clb3clb4clb5*
spc1102ACDK	lic, sat, large	1	1	G1-arrest	
Sld2A	lic, sat, large	1	1	G1-arrest	
Sld3T600A	lic, sat, large	1	1	G1-arrest	
Sld3S622A	lic, sat, large	1	1	G1-arrest	
Sic17A	lic, sat, large	1	1	G1-arrest	
cdh1	0, sat, 0	1	1	G1-arrest	
cln1cln2cdh1	0, sat, 0	1	1	G1-arrest	
spc1104A	rep'd, dup, large	1	1	G2/M-arrest	
pds1	0, 0, large	2	2	T-arrest	
net1cdc15cdh1	0, sat, large	2	2	T-arrest	
cdc15net1	?, ?, large	*	*	Multinucleate: DNA replication and ND, no cell division	
tem1net1	?, ?, large	*	*	Multinucleate: DNA replication and ND, no cell division	